Strictosidine Synthase: Mechanism of a Pictet-Spengler Catalyzing Enzyme†

Justin Maresh[1], Lesley-Ann Giddings[1], Anne Friedrich[1], Elke A. Loris[2], Santosh Panjikar[3], Bernhardt Trout[4], Joachim Stöckigt[2], Baron Peters*[5], and Sarah E. O'Connor*[1]*

*** Corresponding authors: soc@mit.edu; joesto2000@yahoo.com; baronp@engineering.ucsb.edu**

TITLE RUNNING HEAD Mechanism of Strictosidine Synthase

1, Department of Chemistry, Massachusetts Institute of Technology, Cambridge, MA, 02139 USA; 2, Lehrstuhl für Pharmazeutische Biologie, Institut für Pharmazie, Staudingerweg 5, 55099 Mainz, Germany and College of Pharmaceutical Sciences, Zhejiang University, Zijingang Campus, 310058, Hangzhou, China; 3, European Molecular Biology Laboratory, Hamburg outstation DESY, Notkestrasse 85, 22603, Hamburg, Germany; 4, Department of Chemical Engineering, Massachusetts Institute of Technology, Cambridge, MA, 02139 USA; 5, Department of Chemical Engineering, University of California, Santa Barbara, Santa Barbara, CA 93106 USA

Supporting Information

1. Characterization of intermediate from non-enzymatic Pictet-Spengler reaction

NMR spectroscopy

All NMR data were recorded at 15 °C. A combination of COSY, NOESY, ^{1}H and ^{1}H{^{13}N} gradient pulse HSQC, and ^{1}H{^{13}C} and ^{1}H{^{13}C} sensitivity enhanced gradient pulse HMBC[1] pulse sequences were employed to structurally characterize the intermediate on a Bruker AVANCE 600 MHz spectrometer outfitted with an inverse detection cryo-probe. Direct detection ^{13}C-NMR spectra were

recorded on a Varian INOVA 500 MHz spectrometer with a direct-detection probe.

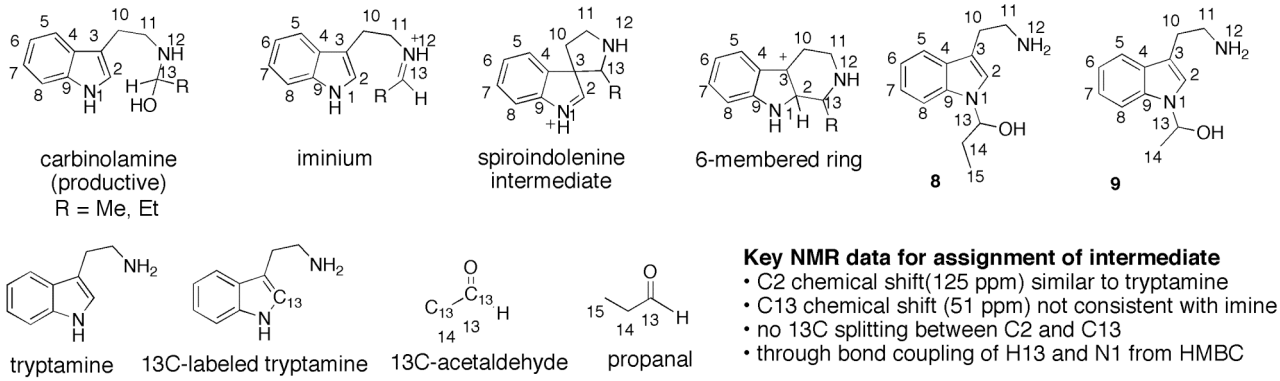

Figure S1. Structures of all proposed intermediates with numbering. Reactants used in these experiments.

NMR assignment of intermediate 9 in reaction mixture

Characterization of the intermediate in the crude reaction was accomplished by using a ^{13}C-labeled acetaldehyde limiting substrate. Reactions were prepared in a 5 mm NMR tube 9:1 D_2O:DMSO-*d6* with 10mM DCl. For reactions with aldehyde in excess: 20 mM acetaldehyde and 0.4 mM tryptamine. For reactions with tryptamine in excess: 20 mM tryptamine and 0.06 mM acetaldehyde. The labeled reactants used were [1,2-^{13}C]-acetaldehyde (Cambridge Isotopes) and [2-^{13}C]-tryptamine.[2] [2-^{13}C]-tryptamine was prepared by decarboxylation of [2-^{13}C]-tryptophan using a previously reported method.[3] Specific peaks corresponding to the intermediate were unambiguously assigned by comparing the kinetics of formation of the NMR peaks with the kinetics of intermediate formation of a parallel reaction evaluated by HPLC. Kinetics were obtained by quantitative ^{1}H-NMR spectroscopy using a 60° flip angle, 4*T_1 delay between scans (longest T_1 = 3.9 seconds), 32 scans averaged.[4] Peaks belonging to the isolated intermediate were spectroscopically identified using a combination of 1D ^{1}H and ^{13}C NMR along with ^{1}H{^{13}C} gradient pulse HSQC.

Labeled reagents (Figure S1) permitted unambiguous assignment of ^{1}H and ^{13}C for positions 2, 13, and 14. Table S1 lists a summary of the assignments from Pictet-Spengler reactions of [1,2-^{13}C]-acetaldehyde with [2-^{13}C]-tryptamine. The C2 chemical shift of the intermediate differed from that of

tryptamine by only 1 ppm (Table S1) suggesting that the intermediate was not the spiroindolenine or the six-membered ring adduct (Figure S1). The upfield C13 chemical shift of 51 ppm was not consistent with an imine species. Distant through-bond coupling was observed for C2 with H13 and H10 in the ^{1}H-{^{13}C} HMBC spectrum of [2-^{13}C]-tryptamine with excess acetal (Figure S2), which was also inconsistent with the productive carbinolamine (Figure S1). To assign the connectivity of this strong coupling, the ^{13}C NMR spectrum for reaction of excess [1,2-^{13}C]-acetal with [2-^{13}C]-tryptamine (Figure S3) revealed a singlet for the intermediate and tryptamine C2 positions, while a doublet resulted from carbon-carbon coupling of C2 with C13 was observed in the product. This result definitively excluded the possibility of a direct bond between C2 and C13 in the intermediate. These data were thus inconsistent with any possible productive intermediate in the Pictet-Spengler reaction. The selective labeling method was sensitive enough to observe species down to 0.5% of the limiting reagent by NMR. No other intermediates were observed by NMR or LC-MS.

NMR assignment of isolated intermediate 8

To confirm these assignments, the intermediate resulting from reaction between propanal and tryptamine, 8, was isolated by preparative HPLC, dried in vacuo, and dissolved in methanol-*d4* and characterized directly. Assigned chemical shifts and correlation data from spectra in Figures S4 – S8 are summarized in Table S2. ^{1}H NOESY spectra (not shown) provided additional support. The ^{1}H and ^{13}C chemical shifts were very similar to the limited positions identified for 9. All C-H couplings were identified in the ^{1}H-{^{13}C} HSQC spectrum (Figure S5); quaternary carbons were identified in the ^{1}H-{^{13}C} HMBC spectrum (Figure S6) and their assigned based on through-bond connectivity. No isolation conditions were found for which the coupling of C13 and OH could be directly observed. However, direct coupling of H13 to N1 was observed in the ^{1}H-{^{15}N} HMBC spectrum of 8 (Figure S7). Furthermore, neither coupling of H13 to the primary amine nitrogen nor evidence of an indole nitrogen proton were observed. In contrast, the identical experiment performed with tryptamine revealed strong coupling of the indole N1 to H2 and H1. The data suggest the structures of compounds 8 and 9, for

reaction of tryptamine with propanal and acetaldehyde respectively (Figure S1). Reversible acylation of indole nitrogen by aldehyde has been reported,[5-7] and our results are consistent with the limited characterization available.

Mass spectrometry of 8

By ESI-MS, (for 8: ESI-TOF: m/z: 201.1393 measured; 201.1392 expected) we were only able to observe the mass fragment indicative of the indole iminium species. Such fragmentations are commonly observed in mass spectra of N-alkylated indoles.[5]

Kinetic behavior of intermediate

The fit of time course kinetics for the intermediate were only consistent with assignment as an off-pathway intermediate (Scheme 1, see also Figure S9 for quality of fit). Taken together, the NMR data and additional results strongly support the structural assignment in Figure S1 for intermediate 8 in the Pictet-Spengler reactions in this study.

Assignment		^{13}C-Shift	Mult.	Coupling	^{1}H-Shift	Mult.	Coupling			
Tryptamine	2	124.46	s	-	7.13	d	181			
Aldehyde	13	208.1	d	39.01	9.41	ddq	175.9	24	2.9	
	14	31.8	d	39.17	1.99	ddd	127.9	6	2.8	
Aldehyde hydrate	13	89.7	d	44.14	5.04	dqd	164.3	4.8	1.7	
	14	24.9	d	44.17	1.13	ddd	126.5	4.9	4.9	
Intermediate	2	123.6	s	-	7.3	‡				
	13	76.4	d	42	5.91	dq	157.5	6.0		
	14	22.9	d	42	1.55	ddd	127.7	5.1	5.1	
Main Product	2	131.78	d	53.3	-	-	-			
	13	50.7	dd	53.3 34.9	4.6*	dm	147.5			
	14	18.5	d	34.9	1.46	dddd	129.6	6.5	4.6	2.1
Side Product A †*	13	64	d	39.5	6.66	dm	155			
	14	21.4	d	39.5	1.9	dm (ddd)	129.6	(5.4)	(5.4)	
Side Product B †*	13	48.9	d	36	5.8	dm	139.7			
	14	21.1	d	36	1.77	dm (ddd)	(134)	(5.1)	(5.1)	

Table S1. Observed chemical shifts from labeling of reactants for Pictet-Spengler reaction. Unless noted, reported J-couplings are for reaction of [2-^{13}C]-tryptamine with excess [1,2-^{13}C]-acetaldehyde. All ^{13}C NMR spectra were proton decoupled during acquisition. Notes: (*) reported J-coupling was observed in reaction of natural abundance tryptamine with [1,2-^{13}C] acetaldehyde; (†) Side product species only observed with tryptamine in 100 fold excess; (‡) due to overlap in 1D spectra, direct coupling was not measured – chemical shift assigned from reaction with unlabeled substrates and HSQC.

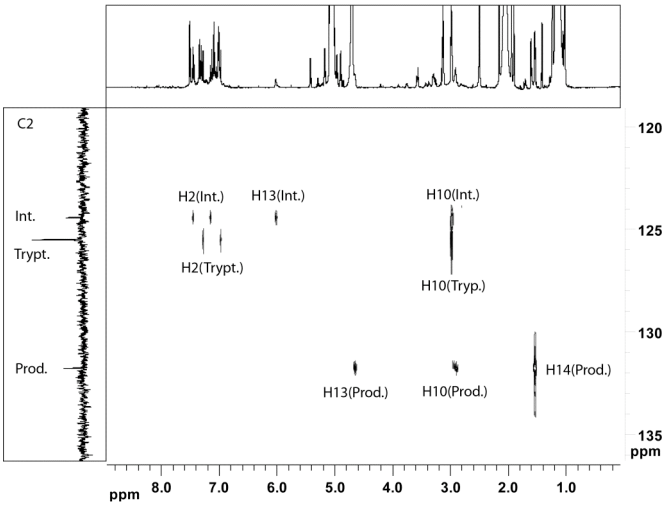

Figure S2. Correlations for position C2 from ^{1}H-{^{13}C} HMBC data for reaction of [2-^{13}C]-tryptamine with excess acetaldehyde. Projections are 1D traces.

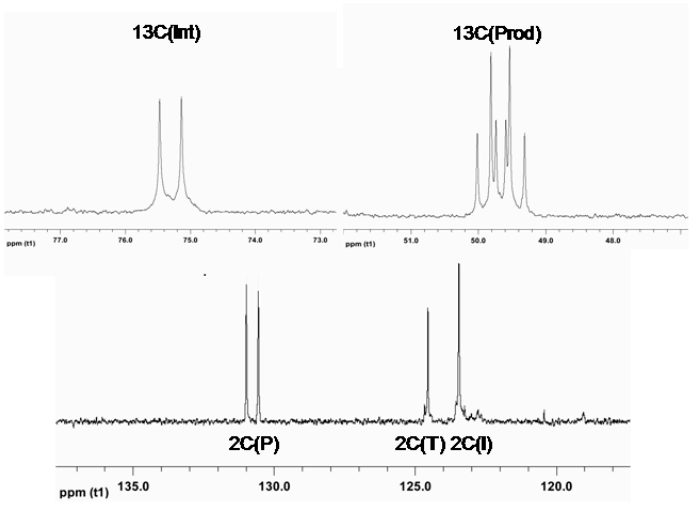

Figure S3. 1D proton decoupled ^{13}C-NMR of reaction of [2-^{13}C]-tryptamine with excess [1,2-^{13}C]-acetaldehyde.

HSQC					HMBC													
	1H			13C														
Index	Shift	Mult.	J	Shift	Index	H2	H3	H4	H5	H6	H7	H8	H9	H10	H11	H13	H14	H15
2	7.32	s		123.4	C2	*								X		X		
3				110.9	C3	X	*		X	X				X	X			
4				128.8	C4	X		*	X	X		X		X				
5	7.58	d	7.83	119.0	C5	X			*		X	X						
6	7.08	t	7.44	120.2	C6					*		X						
7	7.18	t	7.50	122.6	C7				X		*							
8	7.53	d	8.28	111.1	C8							*						
9				137.4	C9	X			X		X		*			X		
10	3.10	t	6.95	24.3	C10	X								*	X			
11	3.22	t	7.50	40.9	C11	X								X	*			
13	5.79	t	6.64	81.2	C13	X										*	X	X
14	2.02-2.16	m		30.3	C14											X	*	X
15	0.88	t	7.40	9.3	C15											X	X	*
	1H			15N														
Index	Shift	Mult.	J	Shift	Index	H2	H3	H4	H5	H6	H7	H8	H9	H10	H11	H13	H14	H15
				152.5	N1	X											X	
12	1.33	br s		28.5	N12									X				

Table S2. Summary of ^{1}H, ^{13}C, and ^{15}N NMR data for observed intermediate 8 for reaction of propanal. ^{1}H-^{13}C and ^{1}H-^{15}N correlations were obtained HSQC data. Quaternary carbons and long-distance heteronuclear coupling were obtained from HMBC data. Not summarized above, are COSY data for which direct coupling of H13 to H14, H14 to H15, H5 to H6, and H7 to H8 were critical to the final assignment of the above resonances. All chemical shifts are in ppm units and all J couplings are in Hz.

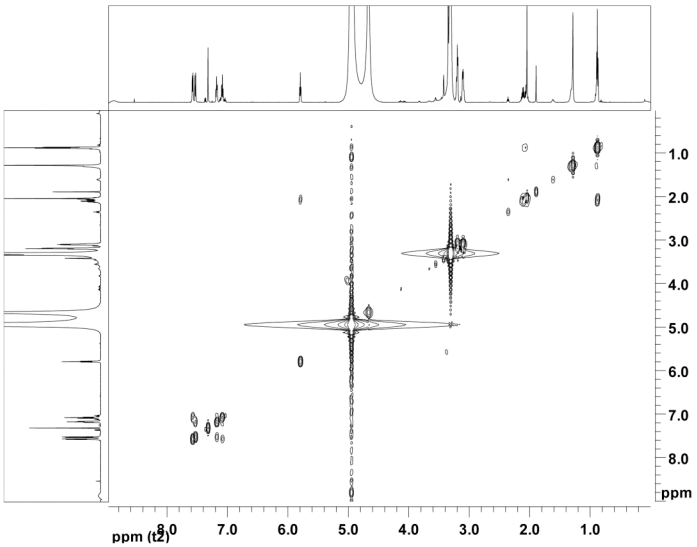

Figure S4. COSY data of intermediate in methanol-*d4* with saturated phosphate buffer pH = 5.0. Resonance frequency for ^{1}H was 600.13269 MHz. Acquisition parameters: standard Bruker gradient pulse selected COSY pulse program, 32 scans, 1024 complex points, 128 t1 increments, 1 second relaxation delay. Processing parameters: zero filling to 512 points in t1, 1° shifted sine bell function applied to t2, 20° shifted sine-squared function applied to t1.

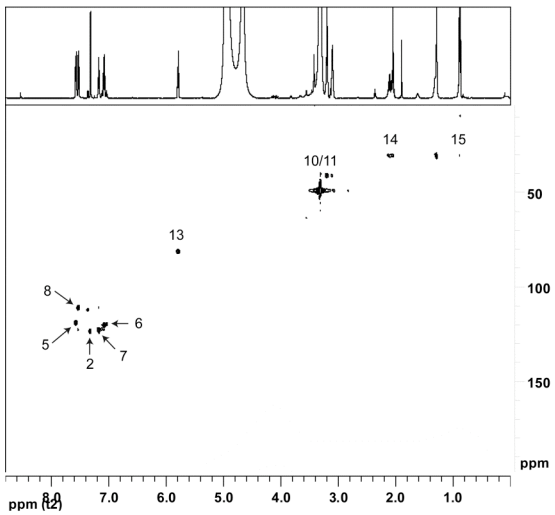

Figure S5. C-H correlations from $^{1}H\{^{13}C\}$ HSQC data of intermediate in methanol-*d4* with saturated phosphate buffer pH = 5.0. The weaker, unlabelled cross peaks near 3.0 ppm and in the aromatic region correspond to tryptamine resulting from decomposition. Acquisition parameters: resonance frequencies for ^{1}H and ^{13}C were 600.13269 MHz and 150.91489 MHz respectively; standard Bruker gradient pulse selected HSQC pulse program, 128 scans, 1024 complex points, 256 t1 increments, 2 second relaxation delay. Processing parameters: zero filling to 1024 points in t1, 90° shifted sine squared bell function applied to both dimensions.

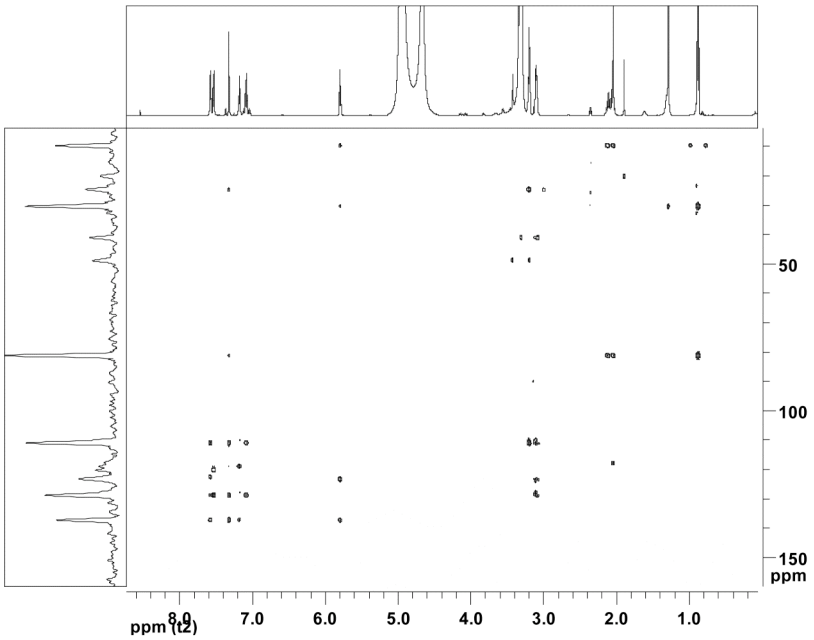

Figure S6. $^{1}H\{^{13}C\}$ HMBC data of intermediate in methanol-*d4* with saturated phosphate buffer pH = 5.0 to identify quaternary carbons and connectivity. Acquisition parameters: resonance frequencies for ^{1}H and ^{13}C were 600.13269 MHz and 150.91489 MHz respectively; sensitivity enhanced gradient pulse HMBC [1] optimized for 6 Hz, 1024 scans, 1024 complex points, 240 t1 increments, 1 second relaxation delay. Processing parameters: zero filling to 2048 points in both dimensions, unshifted sine bell function applied to both dimensions.

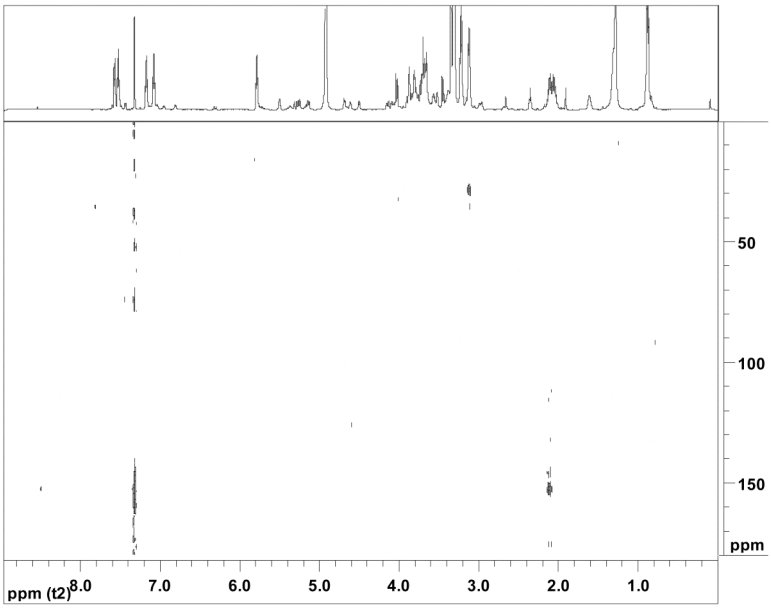

Figure S7. $^{1}H\{^{15}N\}$ HMBC for intermediate in methanol-*d4*. Although this preparation was less pure than the preparations for ^{1}H-^{13}C experiments, the only cross peaks observed were for the intermediate. Acquisition parameters: resonance frequencies for ^{1}H and ^{15}N were 600.46771 MHz and 60.85006 MHz respectively, sensitivity enhanced gradient pulse HMBC [1] optimized for 6 Hz, 4096 scans, 4096 complex points, 86 t1 increments, 1 second relaxation delay. Processing parameters: zero filling to 512 points in t1 dimension, 90° shifted sine squared bell function applied to both dimensions.

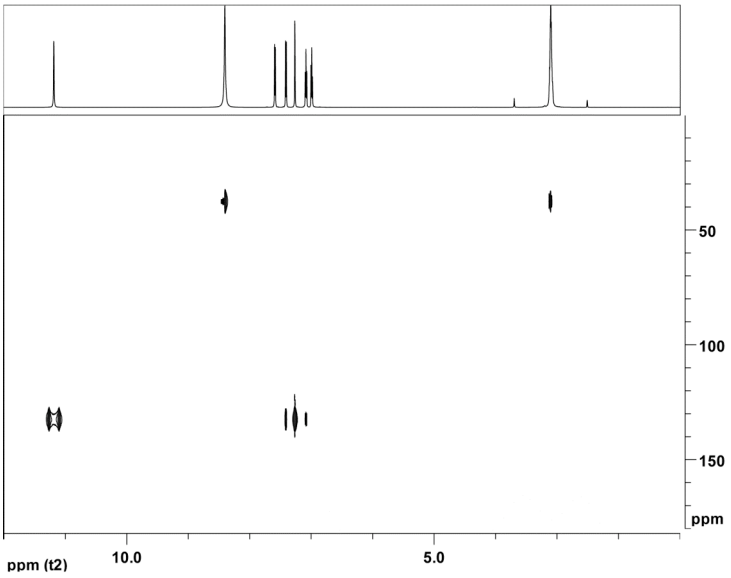

Figure S8. $^{1}H\{^{15}N\}$ HMBC for concentrated tryptamine in DMSO-*d6*. Acquisition parameters: resonance frequencies for ^{1}H and ^{15}N were 600.46771 MHz and 60.85006 MHz respectively, sensitivity enhanced gradient pulse HMBC [1] optimized for 6 Hz, 8 scans, 4096 complex points, 64 t1 increments, 1 second relaxation delay. Processing parameters: zero filling to 256 points in t1 dimension, 90° shifted sine squared bell function applied to both dimensions.

2. Solution reaction kinetics

Representative kinetic data

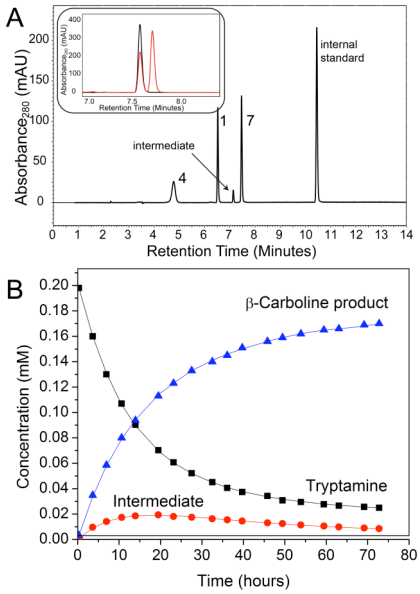

Figure S9. (A) Sample HPLC trace for reaction of tryptamine 1a with propanal 4, (inset)

stereoselectivity of the enzyme for reaction of tryptamine 1a and secologanin 2 is illustrated with the products of the enzymatic (black) and solution (red) reactions, (B) time course data for reaction of tryptamine 1a with propanal 4. Solid lines represents fit to model of Scheme 1 (see Materials and Methods).

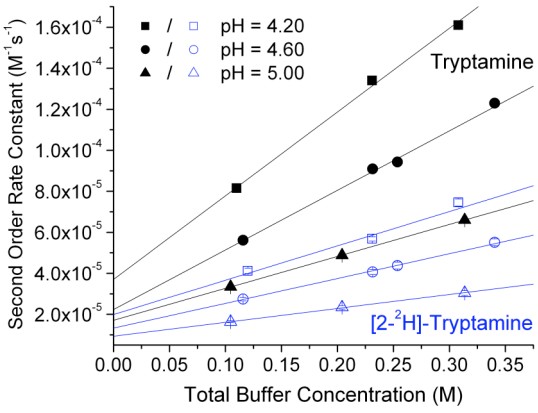

Figure S10. Dependence of second order rate constants on buffer concentration and pH. Data were extrapolated to zero buffer concentration (lines) for calculation of k_o in Equations 2 and 3.

Dependence of rate on acid in solution reaction

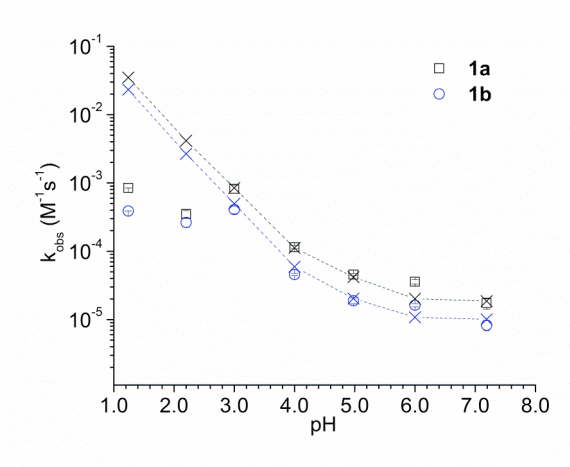

Figure S11. The second order rate constants for the Pictet-Spengler reaction in various buffers. These data indicate that the mechanism of the model reaction studied in acetic acid buffer applies between pH

3.00 – 7.20. Squares and circles represent experimental data. Crosses represent theoretical data predicted by the model in Equation S1 with Bronstead $\alpha = 0.42$. The following 100 mM buffers were used: trifluoroacetic acid (pH = 1.24), maleic acid (pH = 2.20), citric acid (pH = 3.00), formic acid (pH = 4.09), acetic acid (pH = 4.98), citric acid (pH = 6.00), phosphoric acid (pH = 7.19).

To predict k_{obs} in different buffers, k_o was defined: $k_o = k_H[H] + k_{spon}$. The term k_H accounts for specific acid catalysis, k_{spon} is the rate "spontaneous" reaction catalyzed by solvent water. Applying this definition to Equation 7, yields Equation S1.

$$k_{obs} = k_{HA}[AcOH] + k_A[AcO^-] + k_H[H] + k_{spon} \qquad \text{(Equation S1)}$$

The values of k_H and k_{spon} were determined from the slop and intercept of plotting k_o against [H] for the data in Figure 5A. The values of k_{HA} and k_A were the same as those calculated in the text. These constants were determined in acetic acid buffer. However, the catalytic strength of an acid depends on its pKa following the Brønstead relationship ($\log(k_{rxn}) = \text{Constant} + \alpha\ pKa$). Therefore, to predict k_{obs} in buffers other than acetic acid, the value of k_{HA} was adjusted by the literature pKa of the acid following this relationship. We estimated α as 0.42 by treating assuming that the experimentally derived values of $k_H[H^+]$ and k_{spon} represent general-acid catalysis mechanisms with solvent. That is, $k_H[H^+] = k_H[H^+][H_2O]$ and $k_{spon} = k_{spon}[H^+][OH^-]/55.3M$ (assuming hydronium ion pKa = -1.74 and water pKa = 15.57 at 30°C). The adjusted parameters of Equation S1 were applied to the data in Figure S11 (crosses and dotted lines) to predict k_{obs} in each buffer condition by plugging-in the concentrations of the catalytic buffer species.

This model provides satisfactory predictions of k_{obs} in a variety of buffers and pH conditions. The slight deviations from this model curve (particularly in pH 6.00 citrate buffer) are at least partially due to errors in aldehyde concentration since aldehydes in aqueous solution are in equilibrium with their

gem-diol hydrates. This equilibrium is highly dependent on anions which stabilize the hydrated form;[6] anion concentration and composition was not controlled across the different buffers. Despite the fact that we made no effort to measure or correct for deviations in aldehyde concentration, the general-acid catalysis mechanism described by Figure 5, apparently applies between pH 3.00 – 7.20, conditions relevant to our enzyme catalysis studies.

3. pH dependence of Pictet Spengler reaction with N-(omega) methyl tryptamine 5

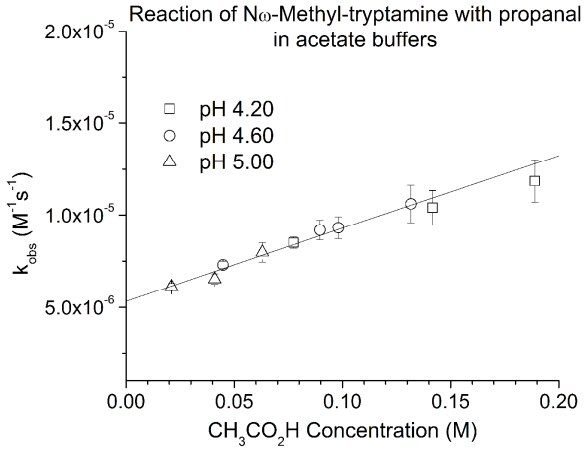

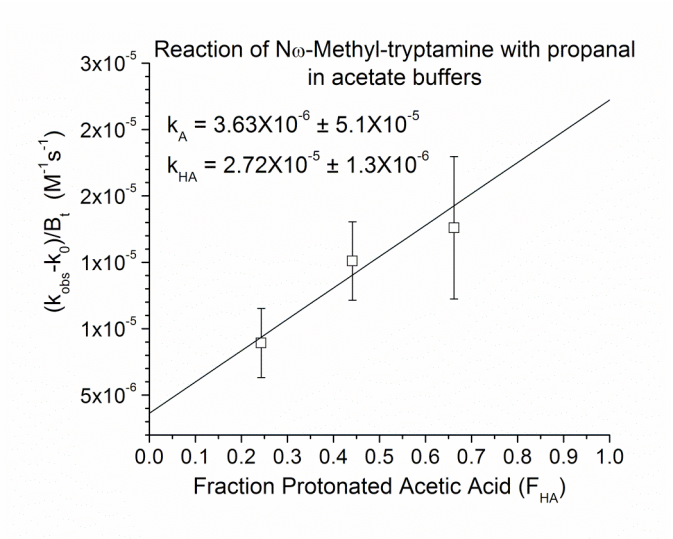

Figure S12. pH dependence of reaction with compound 5 and propanal 4. These data, which indicate that the Pictet Spengler reaction with these substrates is acid catalyzed, are similar to the pH dependence observed with reaction of tryptamine 1a and propanal 4.

4. pH dependence of ^{D}V dependence on pH

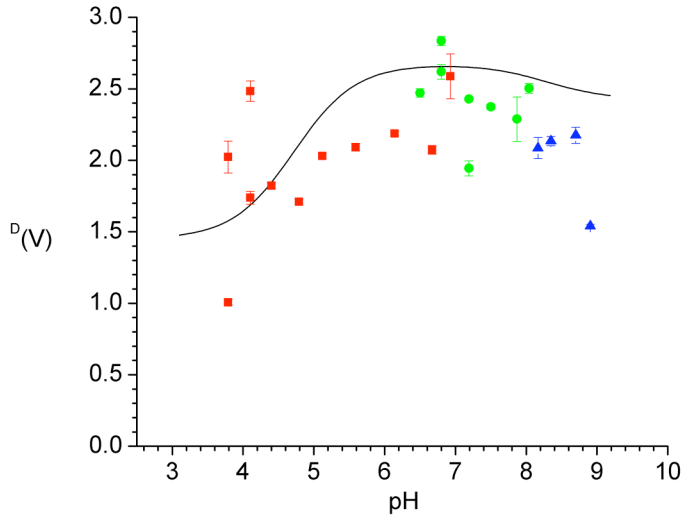

Figure S13. The pH dependence of the kinetic isotope effect ^{D}V for strictosidine synthase. The pH dependence of tryptamine 1a and labeled tryptamine 1b were measured and fit to a diprotic model (see Methods) as shown in Figure 4. The resulting curves were divided to derive ^{D}V, which is shown as a black line in the plot above. Individual KIE values at each pH are also shown for reference. Circles, squares, triangles represent citrate, phosphate and borate buffer conditions (see Methods).

5. Calculated structures of transition states

Stationary point geometries were optimized at the PW1PW91/6-31G* level. Energies (V) and frequencies were also computed at this level and used to compute the zero point (zp) contribution and vibrational free energy at 300K. A single point calculation was performed with the PCM solvent model and a larger basis set 6-31+G* at each stationary point. (The increased basis set had little effect on the relative energies.) The free energy (F) of each species includes the vibrational contribution to the free energy, the zero point correction, and the solvent correction. Differences in the rotational partition functions were neglected for these unimolecular reactions, and differences in the translational partition function are identically zero. All transition states have a single imaginary frequency which is reported

in the chart ($v^{\ddagger}$). The length of the C-C bond being broken/formed in the transition state is also reported ($R^{\ddagger}$).

Finally, we note the rationale for "lumping" some species into a single basin. The structures within each lump of four stable compounds can interconvert within the lump without breaking a bond. The interconversions amount to ring puckerings, sp^3 nitrogen inversions, and boat-chair interconversion. All of these processes should occur quickly, so for kinetic analysis each lump can be treated as a single species. More rigorous lumping strategies are outlined in this reference.[7]

Figure S14. Free energy minima (bottoms of the vertical black lines) and transition states (tops of the arcs connecting the vertical lines) on a plot to show the connectivity of the free energy landscape. Trans and cis refer to isomers of the iminium species, 6-ovr and 6-off refer to the 6-membered ring structure with the methyl group over the indole ring and off of the indole ring respectively. The timescales on the right are from transition state theory and they reflect the timescale for passage through each column from the trans-iminium state.

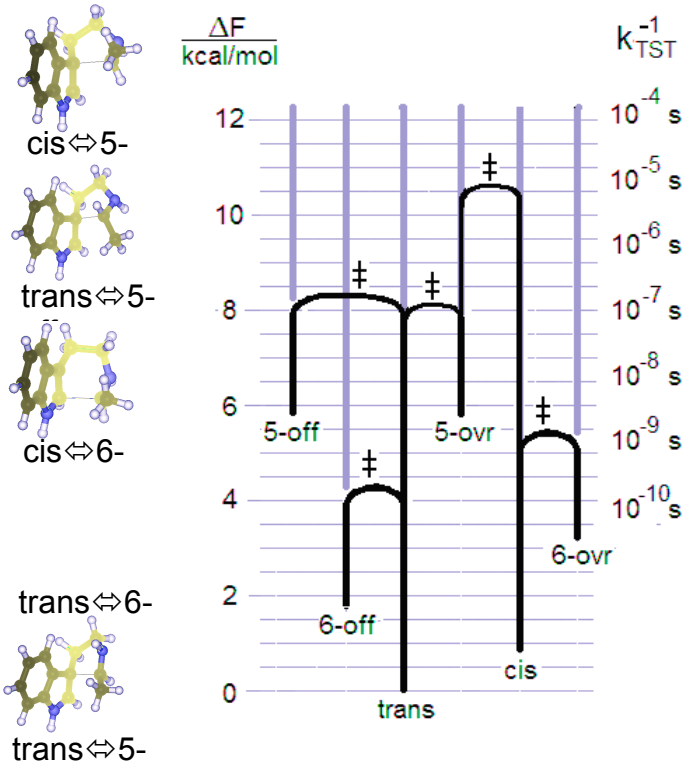

	V	V_{ppm}	V_{ppm+zp}	F	$-kT\ln\Sigma e^{-bF}$	v/cm^{-1}	R /A	Figure 7
Ground States								
Cis	1.42	1.92	1.10	0.85	0.85			**I**
Trans	0.00	0.90	0.00	0.00	0.00			**E**
5ovLax	9.32	4.58	4.71	5.74				
5ovLeq	9.96	5.69	5.95	7.09				
5ovReq	8.38	5.04	5.26	6.38				
5ovRax	9.33	4.65	4.77	5.90				
lumped					5.27			**G**
5offReq	10.16	6.25	6.69	8.17				
5offRax	12.14	5.77	6.07	7.30				
5offLeq	11.48	7.19	7.51	8.87				
5offLax	9.34	4.65	4.97	6.34				
lumped					6.20			**A**
6ovBax	9.85	8.88	9.03	10.40				
6ovBeq	9.93	9.15	9.08	10.17				
6ovCax	2.93	1.13	1.52	3.20				
6ovCeq	5.01	4.50	4.68	6.27				
lumped					3.19			**K**
6offBax	9.49	7.96	7.85	9.18				
6offBeq	9.54	9.41	9.20	10.33				
6offCax	0.06	0.00	0.18	1.81				
6offCeq	2.23	3.25	3.26	4.83				
lumped					1.80			**B**

Transition States								
cis=5offLax	13.80	11.54	11.08	12.43	12.43	253i	2.072	
cis=5ovRax	13.58	9.34	9.01	10.58	10.58	261i	1.978	**H**
cis=6offBax	15.22	14.19	13.71	15.26	15.26	242i	2.071	
cis=6ovCax	7.58	4.29	3.78	5.43	5.43	223i	2.110	**J**
tr=5ovLax	10.45	8.02	7.44	8.13	8.13	250i	1.940	
tr=5offRax	9.98	7.32	6.83	8.33	8.33	217i	1.902	**C**
tr=6offCax	4.46	3.24	2.63	4.30	4.30	225i	2.096	**D**
tr=6ovBax	13.06	11.92	11.30	12.62	12.62	262i	2.016	

Table S3. Tabulation of calculated ground state and transition state energies.

6. References

(1) Cicero, D. O.; Barbato, G.; Bazzo, R. *J. Magn. Reson.* **2001**, *148*, 209-213.

(2) Branchini, B. R.; Prendergast, F. G.; Spencer, G. A.; Hugdahl, J. D.; Ray, B. D.; Kemple, M. D. *J. Labeled Cmpds. Rad.* **1987**, *24*, 637-643.

(3) Hashimoto, M.; Eda, Y.; Osanai, Y.; Iwai, T.; Aoki, S. *Chemistry Letters* **1986**, 893-896.

(4) Rabenstein, D. L.; Keire, D. A. In *Modern Techniques in NMR Spectroscopy and their Application in Chemistry*; Popov, A. I., Hallenga, K., Eds. 1991, p 323-369.

(5) Duffield, A. M.; Beugelmans, R.; Budzikiewicz, H.; Lightner, D. A.; Williams, D. H.; Djerassi, C. *J Am Chem Soc* **1965**, *87*, 805-810.

(6) Cox, B. G.; McTigue, P. T. *Aust. J. Chem.* **1969**, *22*, 1637-1647.

(7) Coxson, P. G.; Bischoff, K. B. *Ind. Eng. Chem. Res.* **1987**, *26*, 1239-1248

Additionally the complete reference for the Gaussian program is:

Gaussian 03, Revision C.02, M. J. Frisch, G. W. Trucks, H. B. Schlegel, G. E. Scuseria, M. A. Robb, J. R. Cheeseman, J. A. Montgomery, Jr., T. Vreven, K. N. Kudin, J. C. Burant, J. M. Millam, S. S. Iyengar, J. Tomasi, V. Barone, B. Mennucci, M. Cossi, G. Scalmani, N. Rega, G. A. Petersson, H. Nakatsuji, M. Hada, M. Ehara, K. Toyota, R. Fukuda, J. Hasegawa, M. Ishida, T. Nakajima, Y. Honda, O. Kitao, H. Nakai, M. Klene, X. Li, J. E. Knox, H. P. Hratchian, J. B. Cross, V. Bakken, C. Adamo, J. Jaramillo, R. Gomperts, R. E. Stratmann, O. Yazyev, A. J. Austin, R. Cammi, C. Pomelli, J. W. Ochterski, P. Y. Ayala, K. Morokuma, G. A. Voth, P. Salvador, J. J. Dannenberg, V. G. Zakrzewski, S. Dapprich, A. D. Daniels, M. C. Strain, O. Farkas, D. K. Malick, A. D. Rabuck, K. Raghavachari, J. B. Foresman, J. V. Ortiz, Q. Cui, A. G. Baboul, S. Clifford, J. Cioslowski, B. B. Stefanov, G. Liu, A.

Liashenko, P. Piskorz, I. Komaromi, R. L. Martin, D. J. Fox, T. Keith, M. A. Al-Laham, C. Y. Peng, A. Nanayakkara, M. Challacombe, P. M. W. Gill, B. Johnson, W. Chen, M. W. Wong, C. Gonzalez, and J. A. Pople, Gaussian, Inc., Wallingford CT, 2004.